

## MAGNETIC THEORIES OF SOLAR FLARES

E. R. Priest  
 Applied Mathematics Department, The University,  
 St Andrews, Scotland

ABSTRACT. The basic processes of evaporation and magnetic reconnection have recently been developed in much greater detail. They may be important in the two main types of flaring event, namely simple-loop flares and two-ribbon flares. The first type could be produced by kink instability, thermal nonequilibrium, or emerging flux. The second type is thought to be the result of an eruptive MHD instability that is either spontaneous or triggered from outside. After the eruption the magnetic field lines that have been blown open reconnect back down in a way that has now been simulated numerically.

### 1. INTRODUCTION

There seem to be two distinct types of flare produced by different physical mechanisms, namely *simple-loop flares* and *two-ribbon flares* (e.g. Pallavicini et al., 1977; Heyvaerts et al., 1977; Priest, 1981). In the one case the magnetic field is static and contains the flare, whereas in the other case the whole magnetic structure goes unstable and blows open. It is this physical classification which is important, rather than any botanical subdivision. There may be exceptions, or it may be shown to be too simplistic in future, but at present it appears to be a helpful subdivision for the theoretical models and it is important to try and seek an overall pattern in the jungle of observations. I recommend that, in future, observers make it clear, if possible, which type of flare they are describing. For instance, it is not sufficient just to refer to a "flare loop", since the physical processes in compact and 'post'-flare loops may well be quite different.

The properties of the two categories of flare (essentially, small flares and large flares) are as follows. Most subflares and flares are of simple-loop type. They consist of a single loop, typically 10 000 km high, with a temperature of  $2 \times 10^7$  K and a density of  $10^{17} - 10^{18} \text{ m}^{-3}$ . The loop brightens in soft X-rays and remains unchanged in position and shape. By comparison, most major events are two-ribbon flares. They take the form of an arcade of hot loops which rises at  $20 \text{ km s}^{-1}$  or more in the initial stages and at only  $0.5 \text{ km s}^{-1}$

later on, reaching an altitude of 100 000 km. The summit density and temperature are about  $10^{17} \text{m}^{-3}$  and  $2 \times 10^7 \text{K}$  at first, falling to  $10^{16} \text{m}^{-3}$  and  $5 \times 10^6 \text{K}$  after a few hours. This type of flare occurs near a dark H $\alpha$  filament which, during the preflare phase, erupts slowly and enhances the soft X-ray emission. Then the eruption suddenly becomes violent and H $\alpha$  knots are produced. Two H $\alpha$  ribbons form and separate, being joined by the rising arcade of 'post'-flare loops. In soft X-rays, simple-loop flares have small volumes, large pressures and short time-scales, whereas two-ribbon flares display the opposite features (Pallavicini et al., 1977). Simple-loop events show at most a single spike ( $\leq 1$  min) in hard X-rays and the energy may be released only at the impulsive phase. Two-ribbon events may sometimes have multiple hard X-ray spikes ( $\geq 5$  min) and the energy release continues through the main phase. They may also produce a coronal transient and are often associated with spot motions, emerging flux and reconnections (Zirin, 1974; Rust, 1976). Two-ribbon flares may be subdivided into: ones that are slow, long-lived and thermal due to the eruption of a quiescent filament (with a weak magnetic field and often no H $\alpha$  emission); and ones that are violent, fast and nonthermal due to a plage filament eruption (with a magnetic field that is strong and complex).

## 2. BASIC THEORY

The fundamental theories of loop flows and magnetic reconnection have recently made great strides. They are possibly important for both types of flare and have entered a stage of sophisticated numerical study.

### 2.1 Loop flows

The thermal response of plasma in a loop to a sudden release of heat has been studied by many authors (e.g. Antiochos and Sturrock, 1976; Somov et al., 1977; Nagai, 1980; Craig, 1981; Wu et al., 1981; Mariska et al., 1982; Doschek et al., 1982; McClymont and Canfield, 1982). The basic approach is to solve the one-dimensional single-(or two-)fluid equations for flow along a rigid flux tube, namely

$$\frac{D\rho}{Dt} + \rho \frac{\partial v}{\partial s} = 0 ; \quad \rho \frac{Dv}{Dt} = - \frac{\partial p}{\partial s} + \rho g \cos \theta ;$$

$$p = R\rho T; \quad \frac{\rho}{\gamma-1} \frac{D}{Dt} \left( \frac{p}{\rho} \right) = \frac{\partial}{\partial s} \left( \kappa_{\parallel} \frac{\partial T}{\partial s} \right) - p \frac{\partial v}{\partial s} - \mathcal{R} + H.$$

Switching on a heat source causes a conduction front and a shock wave to propagate along the loop down to the chromosphere, which is then heated and expands upwards (i.e. *evaporation*). Eventually, the hot plasma cools and *drains* back down, the whole process having oscillations superimposed on it at the sound travel time ( $L/c_s$ ). If the heat input is increased in magnitude by a factor 10 it tends to double the maximum temperature, while smaller loops tend to have lower summit

temperatures and higher summit densities (Nagai, 1980). Also, a heat source near the base rather than the summit has the effect of raising the temperature and pressure there and driving an upflow immediately, rather than after a downflow (i.e. expansion) from the summit.

Difficulties in performing realistic simulations include an adequate treatment of the very narrow transition region and of radiative transfer in the chromosphere. Plasma motions in a flare can be exceedingly complex and of different types. Emerging flux and an erupting filament move up, while plasma drains down the legs. Surges may be ejected from the flare site. Evaporation may be driven by either fast particles or thermal conduction. Thus, when a red or a blue shift is reported, it is important to know what type of motion is being observed.

## 2.2 Magnetic reconnection

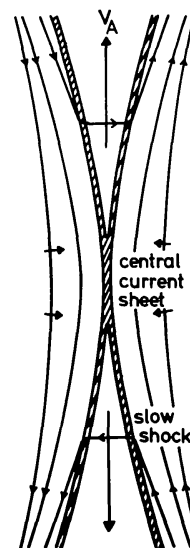
The importance of magnetic reconnection for solar flares has been reviewed by, for instance, Priest (1976, 1981, 1982), Spicer and Brown (1981), Spicer (1981) and Van Hoven (1976, 1981). Reconnection may occur spontaneously by resistive instability in a current sheet or a more generally sheared field (Furth et al., 1963). The linear growth time is typically

$$\tau \sim (\tau_d \tau_A)^{1/2},$$

in terms of the diffusion time ( $\tau_d = d^2/\eta$ ) and the Alfvén travel time ( $\tau_A = d/v_A$ ) across a shear length  $d$ . It is typically days or weeks in the solar corona. The corresponding instability in a flux tube is known as the resistive kink (Coppi et al., 1976), which grows somewhat faster with

$$\tau \sim (\tau_d \tau_A^2)^{1/3}.$$

Figure 1. Petschek's mechanism, in which plasma is heated and accelerated at the slow shocks.



Reconnection may instead be driven during the dynamic formation of a current sheet either due to an ideal magnetic instability (or nonequilibrium) or due to the motion of separate flux systems that are forced together. Whether the reconnection is *spontaneous* or *driven*, its nonlinear development depends critically on the assumed boundary conditions. In many cases it can approach a nonlinear steady state known as Petschek's mechanism (Petschek, 1964; Soward and Priest, 1977, 1982), with a maximum inflow speed of between  $0.1 v_A$  and  $0.01 v_A$ .

We have now entered a period of detailed numerical study of time-dependent reconnection. Ugai and Tsuda (1977, 1979) have considered a magnetic field that is initially antiparallel and at rest. The boundary conditions are free, so that plasma can flow into the numerical box easily. Reconnection is driven by a local resistivity enhancement by a factor 100 so as to give an effective magnetic Reynolds number ( $R_m$ ) of 25. After 20 Alfvén travel-times, the flow evolves to a steady-state configuration, whose first quadrant is shown in Figure 2a. The reconnection rate agrees with the maximum allowable value from Petschek theory and there is a slow shock wave present. Sato and Hayashi (1979) have found similar results when the reconnection is driven by an imposed inflow. The current density structure for all four quadrants (Figure 2b) shows clearly the four slow MHD shocks emanating from the central reconnection region.

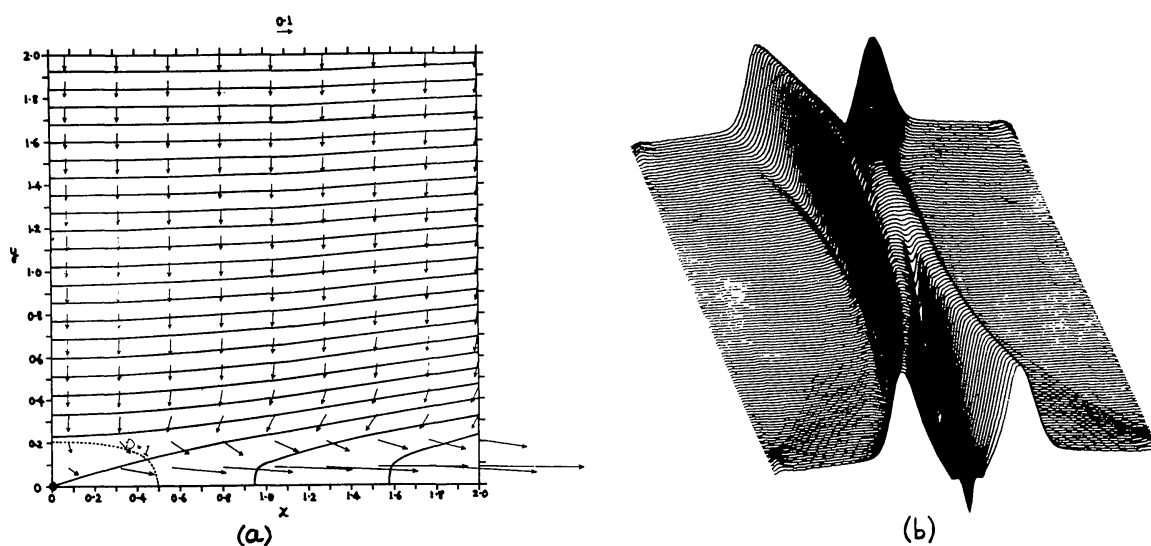


Figure 2. The numerical experiments of (a) Ugai and Tsuda and (b) Sato and Hayashi.

### 3. SIMPLE-LOOP FLARE

#### 3.1 Kink instability

The main problem for understanding the simple-loop flare is to discover how the heat is generated. One possibility is the kink instability, as first analysed in the flare context by Raadu (1972) and later stressed by Spicer (1977). Consider a loop of length  $2L$

with dominant field components  $B_\theta(r)$ ,  $B_z(r)$  that vary with distance ( $r$ ) from the magnetic axis (Figure 3a), so that the amount by which a field line is twisted in going from one end to the other is

$$\Phi = \frac{2LB_\theta}{rB_z} .$$

An important effect for a solar coronal loop is line tying of the loop footpoints in the dense photosphere, which keeps the loop stable until the twist exceeds a critical value ( $\Phi_{\text{crit}}$ ). Raadu (1972), Giachetti *et al.* (1977), Hood and Priest (1979), Einaudi and Van Hoven (1981) found bounds on  $\Phi_{\text{crit}}$ , and later Hood and Priest (1981a) determined the threshold ( $\Phi_{\text{crit}}$ ) exactly as follows.

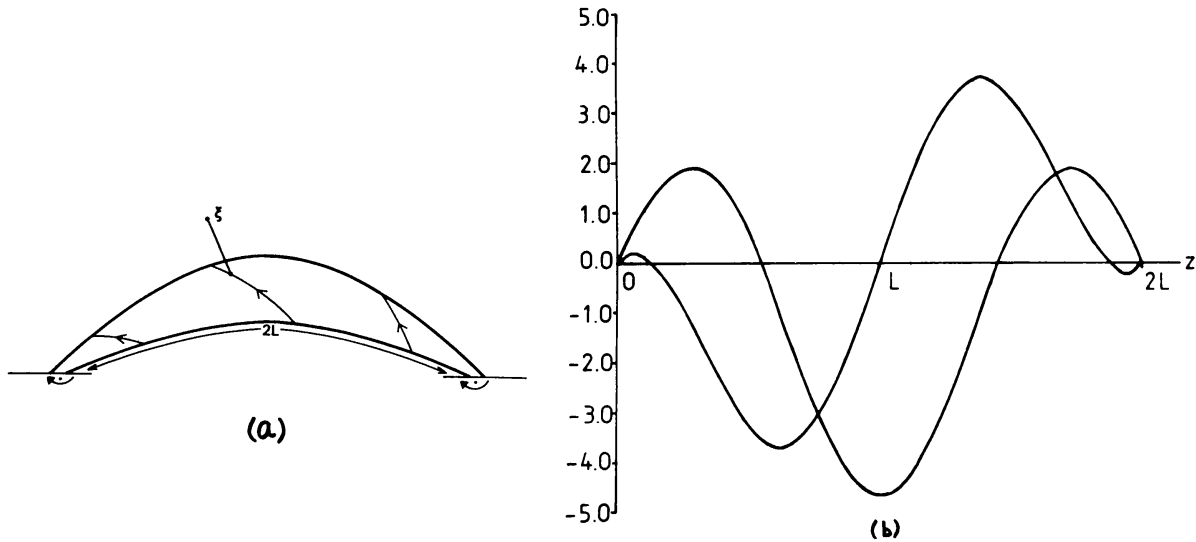


Figure 3. (a) A twisted loop. (b) The unstable perturbation  $\xi_r(z)$ .

A line-tied perturbation of the form

$$\xi = \xi(r, z) e^{i(\theta + \omega t)}$$

is considered, where  $\xi_1$  vanishes at the ends ( $z = \pm L$ ) of the loop and at large distances ( $r \rightarrow \infty$ ). The linearised equation of motion is

$$\rho_0 \frac{\partial^2 \xi}{\partial t^2} = \underline{j}_1 \times \underline{B}_0 + \underline{j}_0 \times \underline{B}_1,$$

where  $\underline{j} = \nabla \times \underline{B}/\mu$  and  $\underline{B}_1 = \nabla \times (\xi \times \underline{B}_0)$ . It reduces to a pair of partial differential equations for  $\xi_r(r, z)$  and  $\xi_\theta(r, z)$ , which are solved numerically to give  $\Phi_{\text{crit}} \approx 2.5\pi$  for a force-free field of uniform twist. The real and imaginary parts of the radial component ( $\xi_r$ ) of the eigenfunction that first gives kink instability are shown in Figure 3b.

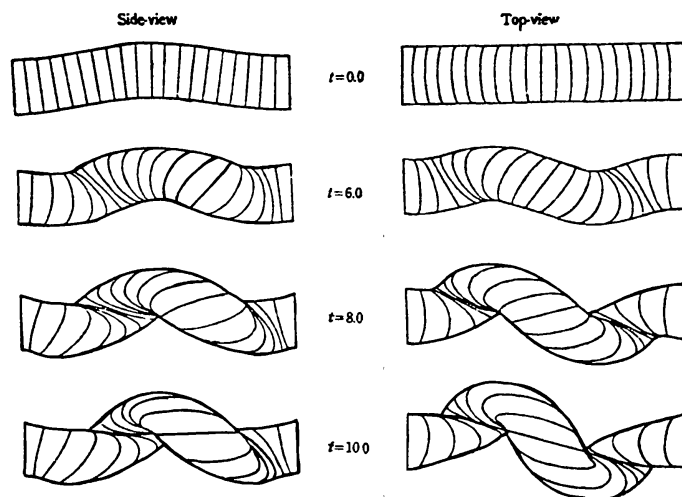


Figure 4. Kinking of a flux tube (Sakurai, 1976).

The present analysis needs to be refined in several ways. The effects of loop curvature, a non-uniform cross-section, shear stabilization and internal modes should be included (e.g. Priest, 1982). The effect of the resistivity in possibly lowering the threshold is important too. Recently, Mok and Van Hoven (1982) have found that line tying completely stabilizes the resistive kink mode and all other resistive modes except for  $m=0$ . This resistive sausage is only unstable when the axial current is large enough and when there is a reversal in the axial magnetic field, which is most unlikely in practice. Thus, it may well be the case that the *ideal* kink modes are the relevant ones for solar flares. Another important task is to follow the nonlinear development in order to see whether the instability saturates or grows explosively. Sakurai (1976) has made a start by considering an infinitely long cylinder of uniform current or force-free field and simulating line-tying roughly by requiring that the axial wavenumber be  $\pi/L$ . His numerical solutions (Figure 4) show how the flux tube rises and twists up. Tubes with a weak twist develop strong helical kinks and rise less than those with strong twist because of the stabilizing tension force from the axial field.

### 3.2 Thermal nonequilibrium

Small X-ray flares may occur when the cool core of a coronal loop loses thermal equilibrium and heats up (Kahler and Kreplin, 1970; Hood and Priest, 1981b), essentially because the radiation is no longer efficient enough to balance the heat sources. This is the case when the heating becomes too large or the loop pressure becomes too small. Even though this is a basically thermal process, the resulting plasma motions may create shock waves which accelerate particles. The role of thermal instability (or nonequilibrium) in causing coronal plasma to cool down and give prominences is well established, and so

it would be surprising if a similar process could not also heat plasma up. For recent numerical simulations of thermal instability in loops, the reader is referred to McClymont and Craig (1982) and McClymont and Canfield (1982).

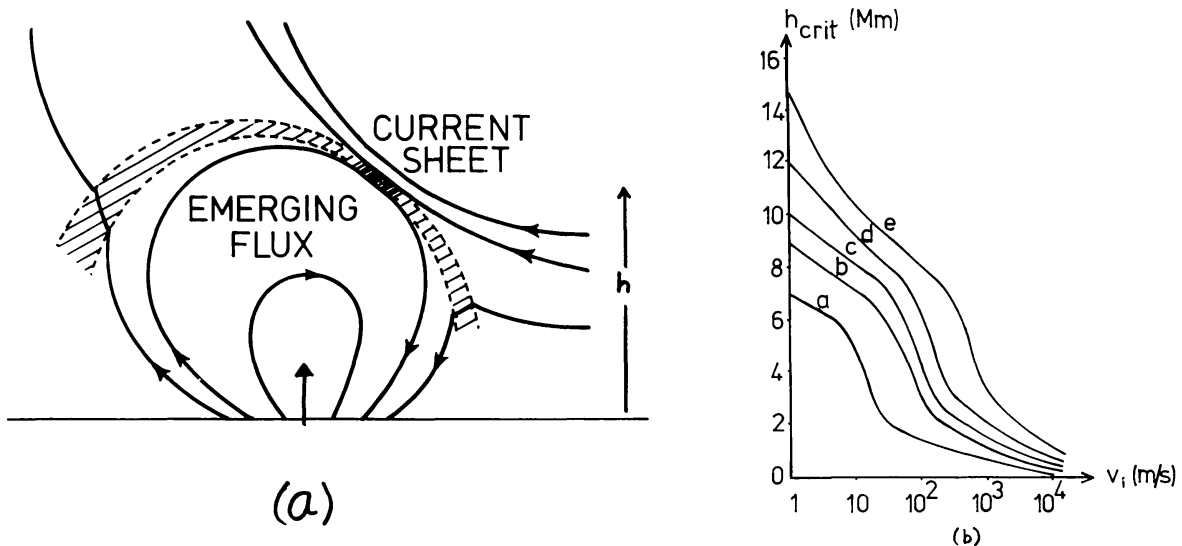


Figure 5. (a) Reconnection of newly emerging flux.  
(b) Critical height for flare onset.

### 3.3 Emerging (or evolving) flux

Topologically separate flux systems may interact when, for instance, new magnetic flux emerges from below the photosphere (Figure 5a) or when satellite sunspots move horizontally. The interaction takes place at a current sheet on the interface between the two systems and leads to a transfer of flux from one system to the other by magnetic reconnection. As more flux emerges or the horizontal motion varies, so the height ( $h$ ) of the current sheet above the photosphere varies. When this height exceeds a critical value ( $h_{\text{crit}}$ ) the current density inside the sheet is so large that the plasma suddenly becomes turbulent and the flare is triggered (Canfield et al., 1974; Heyvaerts et al., 1977; Tur and Priest, 1978). The variation of  $h_{\text{crit}}$  with emergence speed ( $v_i$ ) is shown in Figure 5b for several magnetic field strengths ( $B_i$ ) in G: a, b, c, d, e refer to  $B_i = 10^3, 10^{2.5}, 10^2, 10^{1.5}, 10$ , respectively. It is calculated by solving the energy balance equation inside the reconnecting sheet and deducing the current density there. If  $v_i$  or  $B_i$  is so small that the location of the sheet does not reach  $h_{\text{crit}}$ , then the emerging flux does not produce a flare.

### 4. TWO-RIBBON FLARE

The overall behaviour of the magnetic field during a two-ribbon event is sketched in Figure 6. The initial configuration is a magnetic arcade containing a plage filament along which the magnetic

field is directed. During the preflare phase (Figure 6a) the filament and its overlying arcade start to erupt slowly and stretch out the field lines. Then later (Figure 6b) they erupt much more rapidly, with the field lines starting to reconnect below the filament. In the main phase (Figure 6c) the reconnection continues and creates hot 'post'-flare loops and H $\alpha$  ribbons.

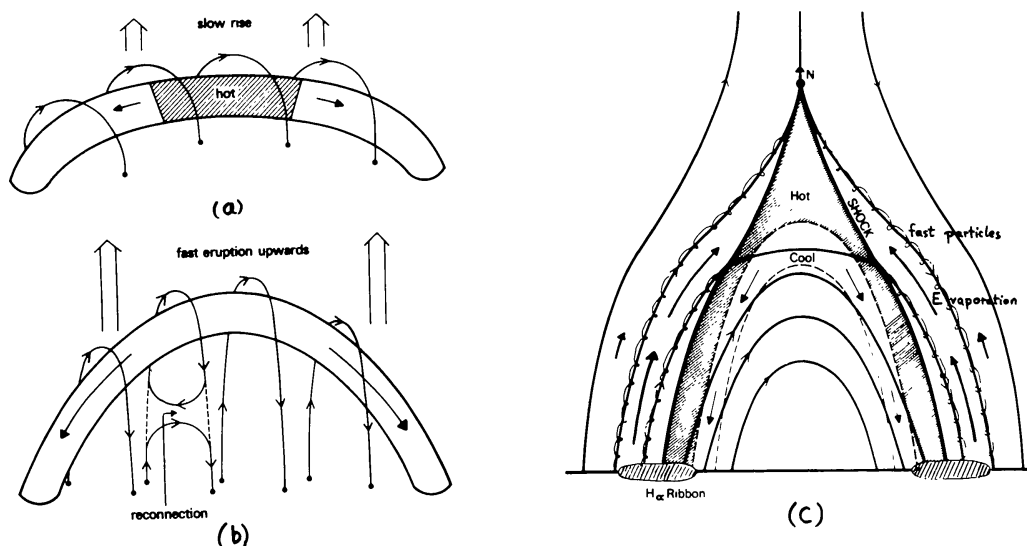


Figure 6. Overall behaviour of a two-ribbon flare.

#### 4.1 Instability of magnetic arcade

In an attempt to find out why a coronal arcade erupts in the first place, the magnetohydrodynamic stability of model arcades has been tested, including the stabilising effect of photospheric line tying (Hood and Priest, 1980; Hood, 1983; Migliuolo and Cargill, 1983). The results show that a simple magnetic arcade with its magnetic axis below the photosphere (so that it does not support a filament) is always stable both to ideal perturbations and, according to Migliuolo and Cargill (1983), also to resistive modes. On the other hand, an arcade whose magnetic axis lies above the photosphere (and so supports a filament), becomes unstable when the height of the magnetic axis (the filament) or the twist in the overlying field are too great.

The filament eruption may therefore be caused by a spontaneous MHD instability when the filament height or field shear become too large. Alternatively, the eruptive instability may be triggered by some other agent such as: emerging flux, which pushes up the filament, tears overlying flux away and forces a large-scale reconnection by lowering the tearing mode time; thermal instability in the filament, which causes the plasma to expand and the filament to rise; a fast magnetoacoustic wave that drives tearing (Sakai and Washimi, 1982).

#### 4.2 Reconnection and creation of 'post'-flare loops

In the main phase after the eruption, the magnetic field closes

down and produces hot loops (Kopp and Pneuman, 1976; Pneuman, 1981), as shown in a section across the arcade in Figure 6c. The neutral point (N) and its trailing slow shocks rise and heat the plasma to  $10^7\text{K}$  or more (Cargill and Priest, 1982), while the  $\text{H}\alpha$  ribbons at the base of the hot loops move apart. Plasma flows upwards ahead of the slow shocks and is heated and compressed at the shocks before cooling and falling back down. The upflow may be partly a reconnection-enhanced solar wind flow and partly an evaporation, driven by heat conduction and fast particles that propagate ahead of the shocks.

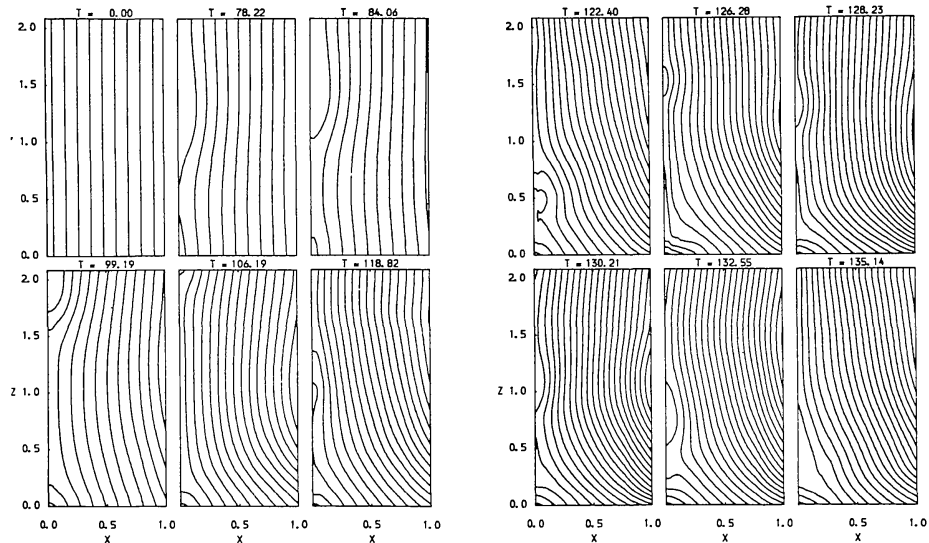


Figure 7. Line-tied reconnection (Forbes & Priest, 1983)

A numerical simulation of the reconnection process has been carried out by Forbes and Priest (1982, 1983). They begin with a vertical magnetic field that reverses at  $x=0$  and is in equilibrium. Line-tied boundary conditions are imposed at the base and free-floating ones at the top and sides. Since  $x=0$  is an axis of symmetry, only half of the magnetic configuration (i.e.  $x > 0$ ) is shown in Figure 7, which presents some results for a magnetic Reynolds number of 150, a plasma beta of 0.1 and a current sheet width that is 0.075 of the box width. The magnetic field lines are shown at several times in units of the Alfvén travel time across the current sheet. First of all, the sheet tears near the base, and then in the nonlinear phase of Petschek-type reconnection the magnetic field closes down and the neutral point rises, while a plasmoid is ejected out of the top (first 4 frames). This process continues, but then the sheet thins (5th frame) and tears again (6th frame), creating a new pair of O- and X-type neutral points. Reconnection at the upper X dominates, and so the O is shot down rapidly (7th frame) and coalesces with the lower X. This process takes place very rapidly at Alfvénic speeds due to the coalescence instability, whereas the formation of the neutral points is on the slower tearing time-scale. Meanwhile, a new pair of neutral points is created (8th frame) and the process repeats.

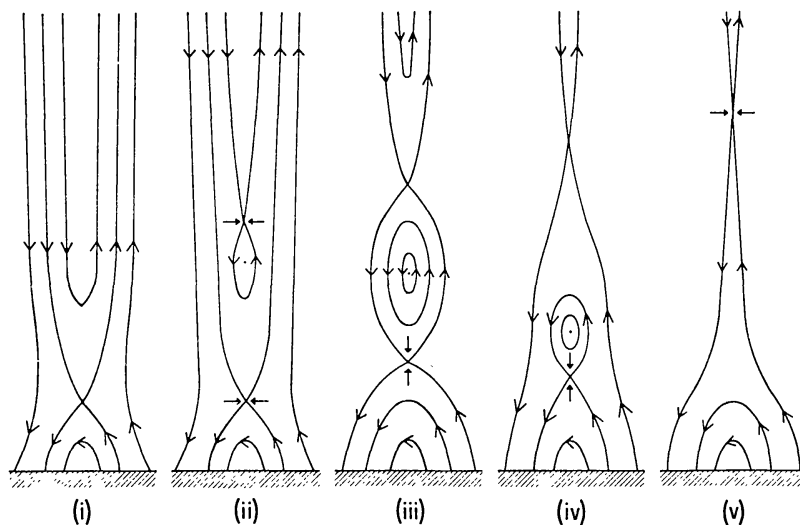


Figure 8. Creation and annihilation of neutral point pairs.

A schematic of the way neutral point pairs are created and annihilated is shown in Figure 8. The extremely rapid coalescence process is associated with strong electric fields and rapid energy release, and it should accelerate particles efficiently. The repetition of the reconnection that has been discovered in the numerical experiment may explain the double (and even multiple) flaring often found in X-rays (e.g. Strong et al., 1982)\*. Another surprise in the simulation is the presence of a fast MHD shock wave below the reconnection region. It slows down the jet of plasma emitted from the region and it may provide significant particle acceleration.

## 5. CONCLUSION

We are at a most exciting stage of flare research as the basic processes of evaporation, MHD instability and magnetic reconnection are being developed and applied to both types of flare. A great deal of progress in our understanding of them should be forthcoming over the next few years. In particular, the details of the instability processes that initiate flares and of the dynamic energy release should be much better understood.

## REFERENCES

- Antiochos, S.K. and Sturrock, P.A.: 1976, Solar Phys. **49**, 359.  
 Canfield, R.C., Priest, E.R. and Rust, D.M.: 1974, Flare-related magnetic field dynamics (ed. Nakagawa, Y. and Rust, D.M.) NCAR, Boulder.  
 Cargill, P.J. and Priest, E.R.: 1982, Solar Phys. **76**, 357.  
 Coppi, B., Galvao, R., Pellat, R., Rosenbluth, M.N. and Rutherford, P.M.: 1976, Sov. J. Plasma Phys. **2**, 533.

\* or Simnett (1982) IAU Colloq. No.71.

- Craig, I.J.D.: 1981, Chapter 5 of *Solar flare MHD* (ed. E.R. Priest), Gordon & Breach, London.
- Doschek, G.A., Boris, J.P., Cheng, C.C., Mariska, J.T. and Oran, S.: 1982, *Ap. J.*
- Einaudi, G. and Van Hoven, G.: 1981, *Phys. Fluids* 24, 1092.
- Forbes, T.G. and Priest, E.R.: 1982, *Solar Phys.* 80,
- Forbes, T.G. and Priest, E.R.: 1983, submitted.
- Furth, H.P., Killeen, J. and Rosenbluth, M.N.: 1963, *Phys. Fluids* 6, 459.
- Giachetti, R., Van Hoven, G. and Chiuderi, C.: 1977, *Solar Phys.* 55, 371.
- Heyvaerts, J., Priest, E.R. and Rust, D.M. 1977, *Ap. J.* 216, 123.
- Hood, A.W. and Priest, E.R.: 1979, *Solar Phys.* 64, 303.
- Hood, A.W. and Priest, E.R.: 1980, *Solar Phys.* 66, 113.
- Hood, A.W. and Priest, E.R.: 1981a, *Geophys. Astroph. Fluid Dyn.* 17, 297.
- Hood, A.W. and Priest, E.R.: 1981b, *Solar Phys.* 73, 289.
- Hood, A.W.: 1983, submitted.
- Kahler, S.W. and Kreplin, R.W.: 1970, *Solar Phys.* 14, 372.
- Kopp, R.A. and Pneuman, G.W.: 1976, *Solar Phys.* 50, 85.
- Mariska, J.T., Boris, J.P., Oran, E.S., Young, T.R., Doschek, G.A.: 1982, *Ap. J.* 255, 783.
- McClymont, A.N. and Canfield R.C.: 1982, submitted.
- McClymont, A.N. and Craig, I.J.D.: 1982, submitted.
- Migliuolo, S. and Cargill, P.J.: 1983, *Astrophys. J.*
- Mok, Y. and Van Hoven, G.: 1982, *Phys. Fl.* 25, 636.
- Nagai, F.: 1980, *Solar Phys.* 68, 351.
- Pallavicini, R., Serio, S. and Vaiana, G.S.: 1977, *Ap. J.* 216, 108.
- Petschek, H.E.: 1964, *AAS-NASA Symp. on Solar Flares*, NASA SP-50, p.425.
- Pneuman, G.W.: 1981, Chapter 7 of *Solar flare MHD* (ed. E.R. Priest), Gordon & Breach, London.
- Priest, E.R.: 1976, *Solar Phys.* 47, 41.
- Priest, E.R.: 1981, *Solar flare MHD*, Gordon & Breach, London.
- Priest, E.R.: 1982, *IAU Colloq.* No. 71, Activity in red dwarf stars.
- Raadu, M.A.: 1972, *Solar Phys.* 22, 425.
- Rust, D.M.: 1976, *Phil. Trans. Roy. Soc. Lond.* A281, 427.
- Sakai, J. and Washimi, H.: 1982, *Astrophys. J.*
- Sakurai, T.: 1976, *Pub. Astron. Soc. Japan* 28, 177.
- Sato, T. and Hayashi, T.: 1979, *Phys. Fl.* 22, 1189.
- Somov, B.V., Spektor, A.R. and Syrovatsky, S.I.: 1977, *Iso. Acad. Sci. USSR Phys. Ser.* 41, 273.
- Soward, A.M. and Priest, E.R.: 1977, *Phil. Trans. Roy. Soc.* A284, 369.
- Soward, A.M. and Priest, E.R.: 1982, *J. Plasma Phys.*
- Spicer, D.: 1977, *Solar Phys.* 53, 305.
- Spicer, D. and Brown, J.C.: 1981, *The Sun as a star* (ed. S. Jordan), p. 413.
- Strong, K. *et al.*: 1982, *Solar Phys.*
- Tur, T.J. and Priest, E.R.: 1978, *Solar Phys.* 58, 181.
- Ugai, M. and Tsuda, T.: 1977, *J. Plasma Phys.* 17, 337.
- Ugai, M. and Tsuda, T.: 1979, *J. Plasma Phys.* 21, 459; 22, 1.

- Van Hoven, G.: 1976, *Solar Phys.* 49, 95.  
 Van Hoven, G.: 1981, Chapter 4 of *Solar flare MHD* (ed. E.R. Priest),  
 Gordon & Breach, London.  
 Wu, S.T., Kan, L.C., Nakagawa, Y., Tandberg-Hanssen, E.: 1981,  
*Solar Phys.* 70, 137.  
 Zirin, H.: 1974, *Vistas in Astron.* 16, 1.

## DISCUSSION

ACTON: Do you predict processes with time scales as short as the time scales of elementary hard X-ray flare burst', say 0.1 sec?

PRIEST: The formation of neutral point pairs occurs on the tearing mode time scale  $(\tau_d \tau_A)^{1/2}$ , which may be typically  $10^2 - 10^3$  sec. The coalescence of islands takes place much faster, namely on the Alfvén time scale  $\tau_A$ , which is a factor of  $R_M^{-1/2}$  shorter and therefore possibly as small as  $10^{-2} - 1$  s. Of course, these values depend very much on the field strength and transverse scale of the structure. What we have done is to identify MHD structures and dynamic behaviour which may lead to particle acceleration. But, having simulated these macroscopic processes, there is a need to consider the microphysics of particle acceleration within them. In particular, I feel it is most important to consider the role of shocks in such acceleration.

KANE: Could you give some specific numbers such as time constants, rate of energy release, etc?

PRIEST: The overall energy release takes place on some multiple of the tearing time, while the additional impulsive energy release at times of coalescence is on the Alfvén time. In order to calculate specific numbers you need to know the plasma parameters such as  $n$ ,  $T$ ,  $B$ ,  $w$ . These results are brand-new and, although we expected the basic reconnection, the appearance of a fast shock and of the creation and impulsive annihilation of neutral point pairs was a great surprise. We hope to put some numbers in and make more quantitative estimates next year during the SMM workshops.

UCHIDA: In calculations by Ugai and others, the implicit non-zero constant  $E$  is equivalent to the assumption of a forced inflow from infinity towards the reconnecting point. In your case, how about this point, and what determines the location of the first and the successively created neutral points? Isn't it due to the effect of the standing fast-mode wave caused by the boundary condition?

PRIEST: The calculations of Sato and Hayashi have an imposed inflow from large distances. By comparison our numerical experiment has free boundary conditions at the sides and the initial state is in equilibrium. It goes unstable and the side boundary conditions allow it to